A Second Mechanism for Aluminum Resistance in Wheat Relies on the Constitutive Efflux of Citrate from Roots[1][W][OA]

Peter R. Ryan*, Harsh Raman, Sanjay Gupta[2], Walter J. Horst, and Emmanuel Delhaize

CSIRO Plant Industry, Canberra, Australian Capital Territory 2601, Australia (P.R.R., S.G., E.D.); EH Graham Centre for Agricultural Innovation, Wagga Wagga, New South Wales 2650, Australia (H.R.); and Institute for Plant Nutrition, University of Hannover, D–30419 Hannover, Germany (W.J.H.)

The first confirmed mechanism for aluminum (Al) resistance in plants is encoded by the wheat (*Triticum aestivum*) gene, *TaALMT1*, on chromosome 4DL. *TaALMT1* controls the Al-activated efflux of malate from roots, and this mechanism is widespread among Al-resistant genotypes of diverse genetic origins. This study describes a second mechanism for Al resistance in wheat that relies on citrate efflux. Citrate efflux occurred constitutively from the roots of Brazilian cultivars Carazinho, Maringa, Toropi, and Trintecinco. Examination of two populations segregating for this trait showed that citrate efflux was controlled by a single locus. Whole-genome linkage mapping using an F_2 population derived from a cross between Carazinho (citrate efflux) and the cultivar EGA-Burke (no citrate efflux) identified a major locus on chromosome 4BL, Xce_c, which accounts for more than 50% of the phenotypic variation in citrate efflux. Mendelizing the quantitative variation in citrate efflux into qualitative data, the Xce_c locus was mapped within 6.3 cM of the microsatellite marker *Xgwm495* locus. This linkage was validated in a second population of $F_{2:3}$ families derived from a cross between Carazinho and the cultivar Egret (no citrate efflux). We show that expression of an expressed sequence tag, belonging to the multidrug and toxin efflux (*MATE*) gene family, correlates with the citrate efflux phenotype. This study provides genetic and physiological evidence that citrate efflux is a second mechanism for Al resistance in wheat.

Because 30% of the world's ice-free land area has a topsoil pH < 5.5, soil acidity remains a serious obstacle for sustainable food production (von Uexküll and Mutert, 1995). Acid soils present a range of stresses to plants, including nutrient deficiencies and mineral toxicities (Matsumoto, 2000; Kochian et al., 2004), but the major limitation to plant productivity on most acid soils is aluminum (Al) toxicity (Taylor, 1988). Soil acidity accelerates the release of Al from minerals such as gibbsite and increases the concentration of the toxic Al^{3+} ions in the soil solution. The Al^{3+} ions can inhibit root growth at micromolar concentrations by disrupting the metabolically active cells at the root apex (Ryan et al., 1993; Sivaguru and Horst, 1998).

Some plant species cope with the toxic Al cations better than others. Even genotypes within certain species vary widely in their ability to grow and yield on acid soils. Wheat (*Triticum aestivum*) shows a large intraspecific variation in Al resistance (Polle et al., 1978; Garvin and Carver, 2003; Stodart et al., 2007; Raman et al., 2008), but establishing the genetic basis for this variation has proved controversial. Reports are generally divided into those that propose a single gene model for resistance and those that argue two or more genes are involved. These conflicting results arise, in part, from the genetic material used. For instance, where near-isogenic lines (NILs) are deliberately developed to differ at a single locus, the trait can be shown to be monogenic. Where different conclusions have emerged from studies of the same parental genotypes, the screening conditions, especially the severity of Al treatment, might have influenced the conclusions. Clearly, our understanding of the genetic control for Al resistance in wheat is incomplete (Garvin and Carver, 2003).

Many studies have proposed that a single major gene can account for most of the variation in resistance in a range of genotypes (Kerridge and Kronstad, 1968; Camargo, 1981; Delhaize et al., 1993a; Luo and Dvorak, 1996; Somers and Gustafson, 1995; Riede and Anderson, 1996; Raman et al., 2005, 2008). Indeed, accumulating evidence is consistent with a major locus on the long arm of chromosome 4D (4DL) being conserved among wheats of diverse origins (Luo and Dvorak, 1996; Riede and Anderson, 1996; Ma et al., 2005; Raman et al., 2005, 2008; Cai et al., 2008). The mechanism of resistance encoded on the 4DL locus has now been attributed to

[1] This work was supported by the Department of Biotechnology in New Delhi, India (S.G.'s travel to CSIRO Plant Industry, Canberra, and his participation in this project).

[2] Present address: ICAR Research Complex for NEH Region, Umiam, 793103 Meghalaya, India.

* Corresponding author; e-mail peter.ryan@csiro.au.

The author responsible for distribution of materials integral to the findings presented in this article in accordance with the policy described in the Instructions for Authors (www.plantphysiol.org) is: Peter R. Ryan (peter.ryan@csiro.au).

[W] The online version of this article contains Web-only data.

[OA] Open Access articles can be viewed online without a subscription.

www.plantphysiol.org/cgi/doi/10.1104/pp.108.129155

the Al-dependent release of malate anions from roots (Delhaize et al., 1993b; Ryan et al., 1995a, 1995b). This model proposes that malate released from roots protects the sensitive growing apices by binding with and detoxifying the harmful Al^{3+} cations in the apoplast (Delhaize et al., 1993b; Delhaize and Ryan, 1995; Ryan et al., 2001; Kinraide et al., 2005). Sasaki et al. (2004) isolated a cDNA from the root apices of an Al-resistant wheat genotype ET8, which encodes a membrane protein (TaALMT1) belonging to a member of a previously uncharacterized gene family (Delhaize et al., 2007). *TaALMT1* is more highly expressed in the root apices of Al-resistant wheat lines than sensitive lines and cosegregates with malate efflux and Al resistance in several mapping populations (Sasaki et al., 2004, 2006; Ma et al., 2005; Raman et al., 2005; Cai et al., 2008; Raman et al., 2008). Heterologous expression of *TaALMT1* in tobacco (*Nicotiana tabacum*) suspension cells and barley (*Hordeum vulgare*) confirmed *TaALMT1* to be an Al-resistance gene (Delhaize et al., 2004; Sasaki et al., 2004). Electrophysiological studies support a model whereby TaALMT1 functions as a ligand-activated and voltage-dependent anion channel to facilitate malate efflux across the plasma membrane of root cells (Ryan et al., 1997, 2001; Zhang et al., 2001, 2008; Yamaguchi et al., 2005; Piñeros et al., 2008). *TaALMT1* homologs recently characterized in Arabidopsis (*Arabidopsis thaliana*; *AtALMT1*) and *Brassica napus* (*BnALMT1*, *BnALMT2*) have also been shown to encode Al-activated malate transport proteins (Hoekenga et al., 2006; Ligaba et al., 2006). Furthermore, a cluster of *TaALMT1* homologs on chromosome 7R of rye (*Secale cereale*; *ScALMT1-M39.1* to *M39.5*) colocalize with a locus-controlling organic anion efflux and Al resistance (Fontecha et al., 2007; Collins et al., 2008).

Other studies propose that Al resistance in wheat is controlled by two or more genetic loci. Examination of ditelosomic lines generated from Chinese Spring identified multiple loci on 5AS, 6AL, 7AS, 2DL, 3DL, and 4DL that were contributing to Al resistance in this moderately resistant genotype (Aniol and Gustafson, 1984; Aniol, 1990; Papernik et al., 2001). Camargo (1981) made multiple crosses between Al-resistant genotypes (Atlas 66 and BH1146) with Al-sensitive genotypes (Tordo and Siete Cerros) and concluded that Atlas 66 possessed two dominant genes for Al resistance and that BH1146 possessed a locus genetically distinct to either of them. Berzonsky (1992) and Tang et al. (2002) similarly concluded that resistance in Atlas 66 was a multigenic trait. Tang et al. (2002) examined two separate BC_3-derived NILs developed with Altas 66 and the Al-sensitive genotypes Chisholm and Century. Atlas 66 possesses the major locus on 4DL, but neither of the NILs was as resistant to Al stress, released as much malate, or was able to exclude Al from their root apices as well as Atlas 66. The authors offered two explanations for these observations: either multiple loci encode for a single mechanism of Al resistance (based on malate efflux) or "modifier loci" operate to enhance the malate efflux encoded by the 4DL locus. This study was unable to support an earlier report that phosphate efflux contributed to the Al resistance of Atlas 66 (Pellet et al., 1996). More recently, a second quantitative trait locus (QTL) for Al resistance in Atlas 66 was localized to the long arm of chromosome 3B (3BL) in a population of recombinant inbred lines derived from Chisholm (Zhou et al., 2007). While the loci on 4DL and 3BL collectively accounted for approximately 50% of the variation, their effects were not additive because expression of the minor QTL on 3BL (accounting for approximately 11% of the variation) was suppressed by the major locus on 4DL (accounting for approximately 45% of the variation). Three significant QTLs for Al resistance on 4DL, 3BL, and 2A were also identified in a recombinant inbred line population from a cross between Chinese wheat lines FSW (Al-resistant) and ND35 (Al-sensitive; Cai et al., 2008). The three QTLs collectively accounted for approximately 80% of the phenotypic variation for Al resistance, and their effects were additive, which contrasts with the report by Zhou et al. (2007). Collectively, these studies present a compelling case for a widespread Al-resistance locus on 4DL, as well as multigenic control of Al resistance in some genotypes of wheat.

The efflux of organic anions is an important mechanism for Al resistance in cereal and non-cereal species (for review, see Ma et al., 2001; Ryan et al., 2001; Kochian et al., 2004). The nature of organic anions released from roots differs between species. Malate is released from Arabidopsis as well as wheat (Hoekenga et al., 2006), citrate is released from maize (*Zea mays*), barley, snapbean (*Phaseolus vulgaris*), and *Cassia tora* (Miyasaka et al., 1991; Pellet et al., 1995; Ma et al., 1997), and oxalate is released from buckwheat (*Fagopyrum esculentum* Moench) and taro (*Colocasia esculenta*; Ma and Miyasaka, 1998; Zheng et al., 1998a). The Al-activated citrate efflux from barley and sorghum (*Sorghum bicolor*) is not controlled by *ALMT1*-like genes but by members of the multidrug and toxin efflux (*MATE*) family of genes. For instance, the Al-activated efflux from sorghum is encoded by *SbMATE* (Magalhaes et al., 2007), and citrate efflux from barley is encoded by *HvAACT1*, also designated as *HvMATE1* (Furukawa et al., 2007; Wang et al., 2007). More recently, Stass et al. (2008) reported Al-activated citrate efflux from roots of the highly resistant Brazilian wheat cultivar Carazinho and suggested that it can influence the Al resistance of triticale (×*Triticosecale* Wittmack) generated from crosses between Carazinho and rye.

This study investigates the efflux of citrate from wheat roots in detail. We provide genetic and physiological evidence that this trait is controlled by a single major locus on the long arm of chromosome 4B (4BL) and that it contributes to Al resistance. We also identify a *MATE* gene whose expression correlates with the citrate efflux phenotype across several genotypes and in a segregating population of $F_{2:3}$ families. These findings are consistent with citrate efflux being a

second major Al resistance mechanism in wheat. To our knowledge, we provide the first physiological evidence that Al resistance in wheat can be a multigenic trait involving distinct mechanisms.

RESULTS

Characterization of Citrate Efflux from Carazinho

We characterized citrate efflux from the roots of the Brazilian genotype Carazinho using intact seedlings and excised root segments. Cumulative organic anion efflux from intact wheat seedlings was monitored through time from the Al-resistant genotype Carazinho and the Al-sensitive genotype Egret. Consistent with the previously characterized mechanism of Al resistance in wheat controlled by *TaALMT1* (see introduction), Carazinho released malate from its roots when exposed to Al but not in control solution (Fig. 1). Carazinho also released citrate and, in contrast to the malate efflux, the rates were comparable in the presence and absence of Al treatment. Egret released little or no malate or citrate in either treatment (Fig. 1).

The variation in malate and citrate efflux along Carazinho and Egret roots was monitored using excised root segments (Fig. 2). As for intact seedlings, malate efflux from Carazinho was activated by Al, especially in the apical zone, whereas citrate efflux was similar in control and Al treatments. Egret showed no changes in the efflux of either anion with Al treatment and very little variation along the root. The effluxes measured in Egret are viewed as background rates that include the residual leakage from the cut surfaces of the excised tissue. Malate efflux decreased steadily back from the root apices of Carazinho so that rates 15 mm back were similar to those measured in Egret. Citrate efflux also decreased behind the apex, but there were indications that the rates back from the apex were slightly larger than in Egret.

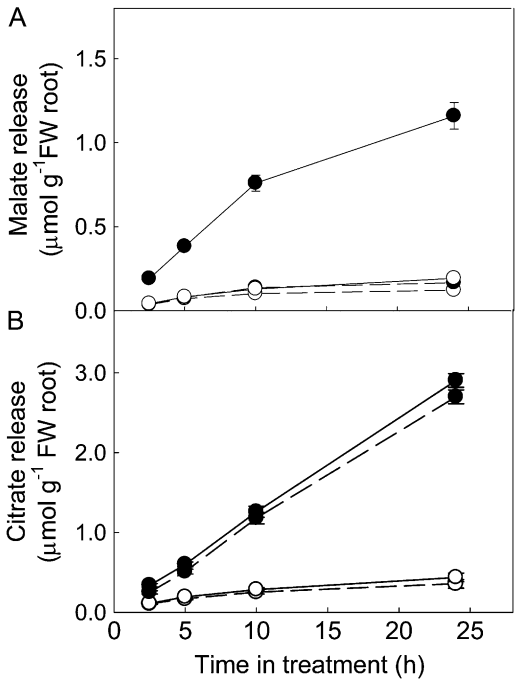

Figure 1. Malate and citrate efflux from intact wheat seedlings. Carazinho (●) or Egret (○) seeds were surface sterilized and grown in conical flasks (12 seeds per flask) on a platform shaker with 20 mL of sterile 0.2 mM $CaCl_2$, pH 4.3. After 6 d, the solution was replaced with similar solutions with (solid line) or without (dashed line) 50 μM $AlCl_3$. Solutions were replaced at each time point. Malate (A) and citrate (B) concentrations were measured with enzyme assays. Data show the mean and SE ($n = 4$).

Citrate efflux from excised root apices was about 10-fold smaller than malate efflux, which contrasts with the findings from intact seedlings. This may be due to a wider distribution of citrate efflux along the root, but it will also be explained, in part, by the more rapid decrease in citrate efflux from the excised root tissues. Malate efflux from excised root apices of Carazinho decreased by only 40% over 6 h in Al treatment, whereas the citrate efflux decreased by 90% over the same period and was unaffected by Al (Supplemental Fig. S1). Subsequent experiments on excised root apices were run for less than 2.5 h.

Citrate Efflux in Other Genotypes of Wheat

Genotypes from China (Chuan Mai 18, Chinese Spring), USA (Atlas 66), Australia (EGA-Burke, Egret, Tasman, ES8, ET8, CD87, Currawong, Vigor 18, Cranbrook, Spica, Kukri, Sunco, Halberd, Janz, Diamondbird), and South America (Carazinho, Toropi, Trintecinco, Maringa, Petiblanco, Veranopolis, Fronteira, BH1146) were tested for citrate efflux to determine how widely the phenotype is distributed. Figure 3 shows that of the 26 genotypes tested here, constitutive citrate release was detected only in Carazinho, Maringa, Toropi, and Trintecinco.

Genetic Control of Citrate Efflux

The genetics of citrate efflux was investigated in two wheat populations segregating for the trait that was derived from crosses between the Brazilian cultivar Carazinho and two Australian cultivars. These included an F_2 population generated from Carazinho and EGA-Burke (low citrate efflux) and a set of $F_{2:3}$ families developed from Carazinho and Egret (low citrate efflux).

F_2 Population Derived from EGA-Burke/Carazinho

Carazinho and EGA-Burke are both Al-resistant cultivars, but Carazinho is more resistant, averaging 50% greater relative root growth over a range of Al concentrations (data not shown). Both parents possess the same resistance allele for *TaALMT1*, the major resistance gene on chromosome 4DL that controls Al-activated malate efflux. EGA-Burke/Carazinho F_1

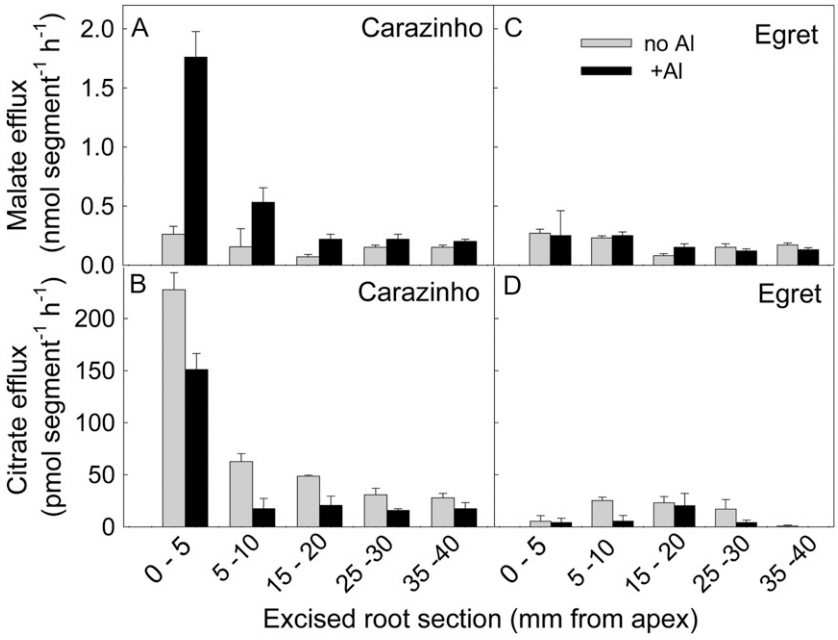

Figure 2. Distribution of citrate and malate efflux along the root. Malate and citrate efflux were measured in excised root segments of Carazinho and Egret in the presence (black bars) and absence (gray bars) of Al. Root segments were excised from 6-d-old seedlings (six segments per replicate). Treatment solutions were 0.2 mM $CaCl_2$, pH 4.3, with or without 50 μM $AlCl_3$. After 2 h, malate (using 0.1 mL of each sample) and citrate (using 0.9 mL) concentrations were measured with enzyme assays. Data show the mean efflux and SE from each section ($n = 3$).

plants show an intermediate phenotype for Al resistance and for citrate efflux, whereas malate efflux was similar in all three lines (Fig. 4). Variation did occur between experiments, and on other occasions, malate efflux was 10% to 20% greater from Carazinho than from EGA-Burke. We also scored 13 BC_1F_1 plants (back-crossed to EGA-Burke) for citrate efflux and found five with low efflux (similar to EGA-Burke) and eight with an intermediate efflux between the parental lines (Supplemental Fig. S2).

Citrate efflux in 132 individual F_2 plants showed a continuous distribution with a peak toward the EGA-Burke parental line (Fig. 5). In 37 of these F_2 seedlings, Al resistance (net root growth in 30 μM Al), malate efflux, and citrate efflux were measured in each seedling. Al resistance varied 2-fold, malate efflux 4-fold, and citrate efflux by 20-fold among the F_2 seedlings. The variation in malate efflux was larger than expected, considering that both parents have the malate efflux phenotype. Although part of this spread may reflect experimental variation, it could also indicate that more than one locus influences malate efflux in Carazinho. This idea would be consistent with Carazinho showing greater malate efflux than EGA-Burke in some experiments. Average malate efflux from the Carazinho and EGA-Burke parental lines was 1.78 $\pm$ 0.10 and 1.35 $\pm$ 0.25 nmol $apex^{-1}$ h^{-1} and citrate efflux was 26.5 $\pm$ 3.7 and 3.0 $\pm$ 1.2 pmol $apex^{-1}$ h^{-1}, respectively (Fig. 6). The average net root growth for the lowest and highest nine seedlings in the distribution was 19.0 $\pm$ 0.5 mm and 30.0 $\pm$ 0.6 mm, respectively, and average citrate efflux from these same plants was 8.2 $\pm$ 1.0 mm and 23.8 $\pm$ 3.7 pmol $apex^{-1}$ h^{-1}, respectively. Al resistance for each seedling was then plotted against the efflux of each anion. Malate efflux was not correlated with Al resistance, and, therefore, was not responsible for the variation in Al resistance in this population (Fig. 6B). By contrast, citrate efflux showed a positive and significant correlation with Al resistance and accounted for 27% of the variation (r = 0.52; Fig. 6C). This result indicates that citrate efflux contributes to Al resistance in this F_2 population over and above the effect of malate efflux.

$F_{2:3}$ Families Derived from Egret/Carazinho

Egret is an Al-sensitive cultivar that possesses neither Al-activated malate efflux nor citrate efflux (see Fig. 1). Egret/Carazinho F_1 seedlings showed a phenotype for citrate efflux that was intermediate between the parental genotypes (Supplemental Fig. 3). Insufficient F_1 seeds were available to measure relative root length (RRL). The malate and citrate effluxes were measured in the presence of 50 μM Al in a set of 45 $F_{2:3}$ families derived from this cross, and the results indicate that these phenotypes segregate independently from one another (Supplemental Table S1). The frequency of the fluxes is summarized in Figure 7. The families were then scored as either being similar to one of the parental genotypes or intermediate between the parents. This analysis generated a ratio of 13:23:9 (low to intermediate to high) for malate efflux and 13:27:5 for citrate efflux (see Fig. 7). Chi-squared tests indicate that these ratios fit a 1:2:1 segregation ($P > 0.05$). Collectively, these results are consistent with malate and citrate efflux each being controlled by single independent loci.

The independent segregation of malate efflux and citrate efflux allowed us to test whether citrate efflux was contributing to Al resistance in the $F_{2:3}$ families. We identified one $F_{2:3}$ family (family no. 30) from the 45 tested that was null for malate efflux and homozy-

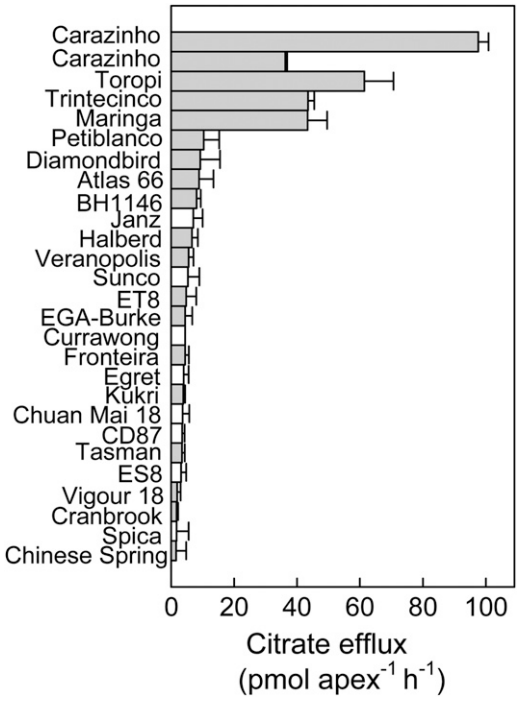

Figure 3. Survey of citrate efflux among different genotypes of wheat. Citrate efflux was measured from root apices excised from 6-d-old seedlings in the absence of Al. Al-resistant genotypes are denoted by the gray bars and Al-sensitive genotypes by the white bars. Two separate measurements for Carazinho are presented to show the variability between experiments. Data show the mean and SE ($n = 3$).

gous for citrate efflux. We also selected additional families that were either null for malate and citrate efflux (family no. 29) or null for malate efflux and segregating for citrate efflux (family nos. 9, 43B, and 44). The Al resistance of these lines was compared with Egret, which is null for malate efflux and citrate efflux (Fig. 8). All four families with citrate efflux were more Al resistant than Egret at one or more of the Al treatments. The single family homozygous for citrate efflux, number 30, showed the greatest level of resistance compared to Egret, with 50% to 100% greater RRL over the range of Al concentrations. We also compared the resistance conferred by citrate efflux with the resistance conferred by malate efflux. Figure 8B shows the RRL in 10 μM Al of Egret and two additional families that are homozygous for malate efflux but null for citrate efflux (nos. 3 and 5; Supplemental Table S1). The malate efflux conferred significantly greater resistance than the citrate efflux. These data are consistent with the relatively lower efflux of citrate compared with malate.

Molecular Mapping and Validation of *Xce$_c$*

Because Chinese Spring does not show the citrate efflux phenotype (see Fig. 3), we were unable to map this trait to a physical map using deletion lines. Instead, the locus conditioning citrate efflux, *Xce$_c$*, was tagged by whole-genome linkage mapping. DNA of the Carazinho and EGA-Burke parental lines and 67 F_2 individuals was analyzed with the diversity microarray technology (DArT). DArT analysis identified 676 polymorphic markers covering all 21 chromosomes of the wheat genome, except 5D (data not shown). A skeleton linkage map was used to find a genomic region associated with citrate efflux. Single marker regression analysis identified a major QTL, *Qce$_c$-4BL*, on the long arm of chromosome 4B that explained more than 50% of the phenotypic variation for citrate efflux. The association between DArT markers and citrate efflux was highly significant ($P < 0.0001$), with a likelihood ratio statistic (LRS) of 46 (Table I; Fig. 9; Supplemental Fig. S4). Interval mapping indicated that *Qce$_c$-4BL* is delimited by DArT

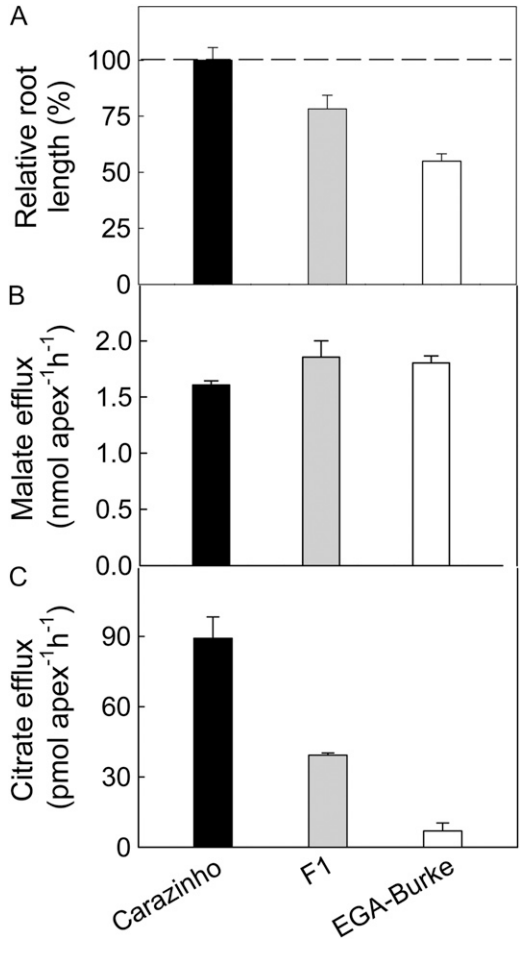

Figure 4. Phenotypes of Carazinho, EGA-Burke, and their F_1 progeny. RRL (A) was calculated from net root growth after 4 d in 0 and 30 μM Al ($n = 7$). To account for the accumulation of errors associated with deriving RRL, the errors were calculated as follows: $SE_{RRG} = RRG\ [(SE_x/x)^2 + (SE_y/y)^2]^{1/2}$, where x and y represent the mean net root length in the control treatment and the mean net root length in the Al treatment. Malate (B) and citrate (C) efflux from excised root apices were measured in the presence of 50 μM Al. Data show the mean and SE ($n = 3$).

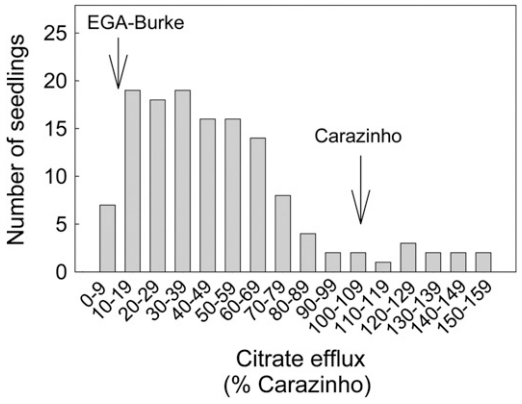

Figure 5. Frequency distribution of citrate efflux among F_2 seedlings. Citrate efflux was measured in root apices excised from 132 F_2 6-d-old seedlings derived from EGA-Burke/Carazinho (four to five apices per seedling). Carazinho was included in each experiment to account for the variation between experiments. The apices were washed and treated with 1 mL of 0.2 mM $CaCl_2$, pH 4.3, for 2 h on a shaker. The data are presented as a percentage of the efflux from Carazinho seedlings and grouped into bins as shown. Mean values for the parental lines are indicated.

markers *Xwpt-8397/Xwpt-8292* with *Xwpt-8397* explaining most of the phenotypic variation for citrate efflux in this population. Marker analysis confirmed that citrate efflux was inherited from the Carazinho parent.

DArT markers are dominant and, therefore, cannot distinguish heterozygotes in segregating populations. Codominant markers are more useful for marker-assisted selection, so we mapped the *Qce$_c$-4BL* region using microsatellite markers, also called single sequence repeat markers (SSR), specific to chromosome 4B. SSR markers *Xwmc349*, *Xbarc163*, *Xgwm251*, *Xgwm495*, *Xgwm513*, and *Xbarc340* were polymorphic in the F_2 population and were used to construct a linkage map of chromosome 4B. Regression analysis revealed a highly significant QTL *Qce$_c$*-4BL ($P < 0.001$) for citrate efflux, with SSR marker *Xgwm495* detecting 51% of the phenotypic variation for citrate efflux (Table I; Supplemental Fig. S4). Integration of SSR and DArT marker data with citrate efflux phenotypes for the EGA-Burke/Carazinho F_2 population revealed that the *Xce$_e$* was flanked with *Xgwm495* and *Xwpt-8397* loci (Fig. 9; Table I).

The two polymorphic SSR markers closely linked with *Xce$_c$*, *Xgwm495* and *Xgwm513*, were further validated in an independent $F_{2:3}$ population derived from Egret/Carazinho. These markers predicted 96% and 91%, respectively, of phenotypic variation for citrate efflux in this population.

We also investigated the linkage between Al resistance and citrate efflux in the F_2 seedlings from EGA-Burke/Carazinho (see Fig. 6). The *Xce$_c$* locus conditioning citrate efflux showed a significant effect on net root growth ($P > 0.05$) and explained 56% of phenotypic variance in this phenotype in the F_2 population, which is consistent with the results presented in Figure 6. This result indicates that while the contribution of citrate efflux to Al resistance is smaller than the contribution from malate efflux (see Fig. 8), its effect is significant and additive.

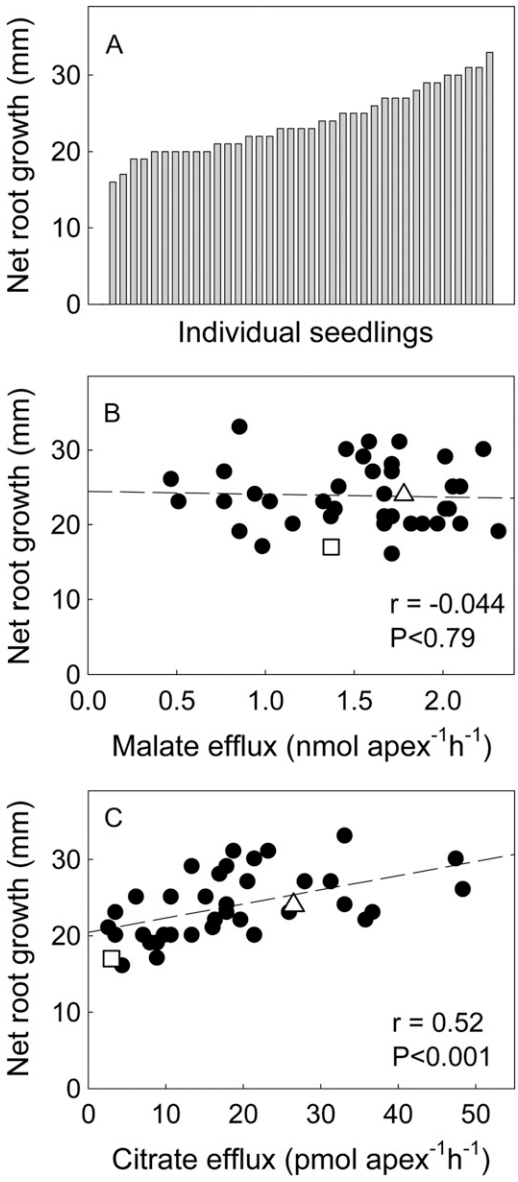

Figure 6. Net root growth and organic anion efflux from F_2 seedlings derived from EGA-Burke/Carazinho. A, Net root growth was measured after 4 d in nutrient solution with 30 μM $AlCl_3$. The seedlings were moved to a control solution and allowed to recover for 3 d. Root apices were then excised from the seedlings (four to five apices per seedling), washed, and treated with 1 mL of 0.2 mM $CaCl_2$, pH 4.3, on a shaker. After 2 h, 0.1 mL of each sample was used for malate assays (B) and 0.9 mL was dried down for citrate assays (C). The triangles in B and C indicate the mean values for the Carazinho parent and the squares indicate the mean values for the EGA-Burke parent. The dashed lines indicate linear regressions with regression coefficients shown.

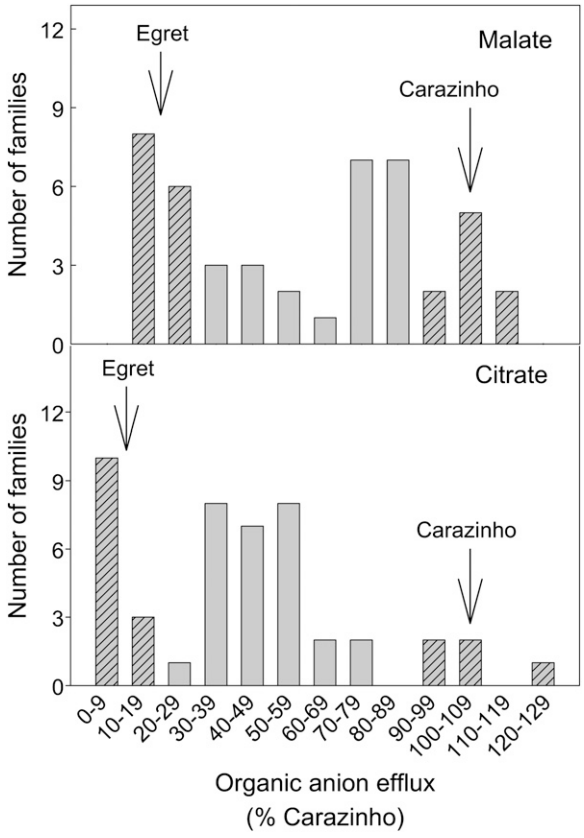

Figure 7. Frequency distribution of malate and citrate efflux from $F_{2:3}$ families derived from Egret/Carazinho. Six to eight seedlings from each of the 45 $F_{2:3}$ families were grown in nutrient solution for 6 d. Measurements of citrate efflux were either made separately on the individual seedlings in each family and the average value used to represent the family, or root apices were bulked from all seedlings (two apices per seedling) and a single bulked sample was measured per family. The data are presented as a percentage of Carazinho seedlings and grouped into bins as shown. Carazinho was included in each experiment to account for the variation between experiments. The hatched bars were scored as being similar to either of the parental genotypes (arrows) to estimate the segregation ratios.

Citrate Efflux Cosegregates with Expression of a *MATE* Gene on Chromosome 4BL

Several SSR markers closely linked with Xce_c have been mapped with the Chinese Spring deletion lines. Markers *Xgwm513* and *Xgwm251/Xbarc163* are allocated to 4BL-5 (fraction length C to 0.71) and 4BL-1 (fraction length 0.86–1.00), respectively (http://wheat.pw.usda.gov/cgi-bin/graingenes; Sourdille et al., 2004). This region (4BL-1 fraction length 0.71–0.86) also includes a wheat EST (GenBank accession no. BE605049) that shows a predicted 94% amino acid sequence identity with a *MATE* gene from barley, *HvAACT1*, also designated *HvMATE1* (Furukawa et al., 2007; Wang et al., 2007). *HvAACT1* controls Al resistance in barley by facilitating Al-activated citrate efflux (Furukawa et al., 2007). Primers to an EST (GenBank accession no. BE498331) representing the putative 3′ end of a wheat gene encoding the MATE located at 4BL (*TaMATE1*) were used to quantify gene expression by real-time PCR (qRT-PCR) in all genotypes listed in Figure 3. *TaMATE1* expression was detected only in the four genotypes showing citrate efflux (Carazinho, Toropi, Maringa, and Trintecinco). We then tested *TaMATE1* expression in the $F_{2:3}$ families derived from Egret/Carazinho. Families with *TaMATE1* expression below the limits of detection were also null for citrate efflux (Fig. 10; Supplemental Fig. S5). All other $F_{2:3}$ families tested showed citrate efflux and detectable *TaMATE1* expression.

DISCUSSION

This study has identified a second mechanism of Al resistance in wheat that relies on citrate efflux. We show that citrate efflux is controlled by a single codominant locus on chromosome 4BL. The first mechanism relies on malate efflux and is controlled by the *TaALMT1* gene on chromosome 4DL (Delhaize et al., 1993b; Ryan et al., 1995b; Raman et al., 2005). Our results demonstrate that Al resistance is a multigenic trait in some genotypes and that these genes do not necessarily act by modifying the function of TaALMT1.

Stass et al. (2008) first reported citrate efflux from the roots of Carazinho while investigating the Al resistance of triticale. They found that citrate was activated by Al treatment and that the wheat parent could influence the Al resistance of progeny from wheat/

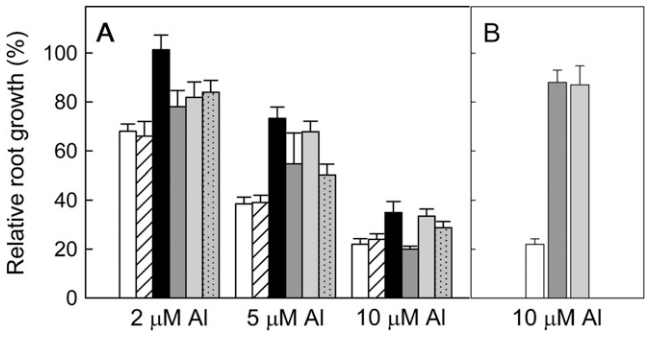

Figure 8. RRL of $F_{2:3}$ families compared to Egret. A, RRL was measured in Egret (white) and five $F_{2:3}$ families. The identities and phenotypes of the $F_{2:3}$ families are as follows: null for malate and citrate efflux (no. 29, white hatched), null for malate and homozygous for citrate efflux (no. 30, black), and null for malate efflux and segregating for citrate efflux (no. 9, dark gray; no. 44, light gray; no. 43B, gray dotted). RRL was calculated by measuring net root growth in 10 seedlings for each line in four Al treatments (0, 2, 5, and 10 μM $AlCl_3$). B, RRL was measured in Egret (white) and two $F_{2:3}$ families that are null for citrate efflux and homozygous for malate (no. 3, dark gray; no. 5 light gray). RRL was calculated by measuring net root growth in 10 seedlings for each line in 0 and 10 μM Al treatments. Data show the mean and SES. SES were calculated using the formula presented in the legend to Figure 4.

Table I. *DArT and SSR markers closely linked with a major QTL for citrate efflux*

The QTL was identified on the long arm of chromosome 4B (*Qce$_c$-4BL*) in an F_2 population derived from EGA-Burke/Carazinho. Linked markers were determined using simple regression analysis (Manly et al., 2001).

DArT Marker Locus	Citrate Efflux		SSR Marker Locus	Citrate Efflux	
	LRS[a]	R^{2b}		LRS	R^2
XwPt-8291	20.1	26	*Xwmc349*	26.5	33
XwPt-6209	28.1	34	*Xbarc163*	30.4	37
XwPt-8796	30.0	36	*Xgwm251*	41.6	46
XwPt-8397	46.0	50	*Xgwm495*	47.1	51
XwPt-8292	14.6	20	*Xgwm513*	42.2	47
			Xbarc340	43.9	48
LRS ($P < 0.05$)[c]	13.8			13.8	
LRS ($P < 0.001$)[c]	21.1			24.3	

[a]LRS value for the association of the trait with the locus. [b]R^2, Phenotypic variance (%) of citrate efflux explained by a QTL. [c]Significance thresholds for the statistics were estimated with 1,000 permutations.

rye crosses. The current study provides a detailed characterization of citrate efflux from wheat roots. We have extended the work of Stass et al. (2008) by demonstrating that citrate efflux actually occurs constitutively in Carazinho and several other highly Al-resistant Brazilian cultivars. This finding contrasts with the citrate efflux characterized in other cereal species such as barley, sorghum, and maize where the citrate efflux is activated by Al in much the same way that malate efflux is activated from Al-resistant wheat plants (Pellet et al., 1995; Furukawa et al., 2007; Magalhaes et al., 2007). We show that the expression of an EST from the MATE family, designated here as *TaMATE1*, is greater in genotypes with high citrate efflux than in genotypes with low efflux and is correlated with citrate efflux in 45 $F_{2:3}$ families segregating for this trait. The close similarity of *TaMATE1* with *HvAACT1*, a MATE gene that controls citrate efflux in barley, identified this gene as a candidate controlling the citrate efflux phenotype in wheat.

Our conclusion that citrate efflux is controlled by a single codominant locus relies on two results: (1) the segregation of citrate efflux in $F_{2:3}$ families (Egret/Carazinho) is consistent with a 1:2:1 ratio (low to intermediate to high); and (2) whole-genome mapping identified a single highly significant QTL on 4BL in an F_2 population derived from EGA-Burke/Carazinho as well $F_{2:3}$ families derived from Egret/Carazinho. Distribution of citrate efflux in F_2 plants did not show the expected 1:2:1 segregation but instead produced a skewed distribution toward the EGA-Burke parent. The difficulty in scoring this trait on single seedlings could have obscured the underlying inheritance. The observed bias of data toward the lower fluxes is consistent with some loss of sensitivity in the measurements. The 4-fold variation in malate efflux in this F_2 population was unexpected, because both genotypes possess the malate efflux phenotype controlled by *TaALMT1*. This may be explained, in part, by experimental error, but it could also indicate that other loci contribute to this phenotype in Carazinho.

Citrate efflux from excised root apices of Carazinho is about 10-fold smaller than malate efflux, while in intact seedlings, the efflux of citrate and malate are comparable. At least part of this discrepancy is likely to be due to the faster decrease in citrate efflux from excised root tissue compared to malate efflux (Supplemental Fig. S1), which means the citrate efflux from excised tissue becomes relatively smaller the longer the measurements are made after excision. We also argue that a comparison between Carazinho and Egret indicates that the citrate efflux extends farther along the root than malate efflux (Fig. 2). Nevertheless, tricarboxylic anions such as citrate form stronger complexes with Al than dicarboxylic anions such as malate (Hue et al., 1986), and a relatively small efflux of citrate from the root apices could afford significant protection from Al stress. Growth experiments support this idea by showing that citrate is approximately 8-fold more effective than malate at ameliorating the inhibition of root growth by Al (Delhaize et al., 1993b; Ryan et al., 1995b; Zheng et al., 1998b; Zhao et al., 2003).

Our conclusion that citrate efflux contributes to Al resistance relies on three results: (1) Al resistance in a population of F_2 plants (EGA-Burke/Carazinho) was significantly correlated with citrate efflux; (2) Al resistance was linked with *Xce$_c$*, the citrate efflux locus on 4BL; and (3) $F_{2:3}$ families (Egret/Carazinho) that displayed citrate efflux were more Al resistant than Egret and another family that did not show citrate efflux. Further experiments are required to confirm that these citrate and malate mechanisms are additive. The intermediate phenotypes of the EGA-Burke/Carazinho F_1 plants (both of which show malate efflux) and the correlation between citrate efflux and Al resistance in the F_2 seedlings also support this idea. Therefore, citrate efflux does contribute to the Al resistance of

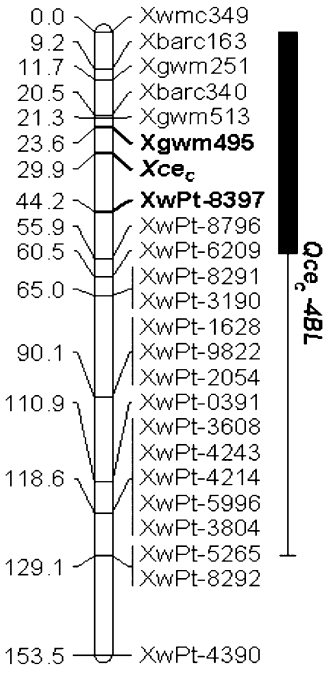

Figure 9. Mapping the *Xce$_c$* locus. Graphical representation of an integrated map based upon DArT and SSR markers showing the position of a major locus conditioning citrate efflux on the long arm of chromosome 4B in an F_2 population from Carazinho (Al resistant, positive for citrate efflux) and EGA-Burke (Al resistant, negative for citrate efflux). The bold marker loci *Xgwm495* (SSR) and *Xwpt-8397* (DArT) flank the *Xce$_c$* for citrate efflux and account for 51% and 50% of phenotypic variation in citrate efflux, respectively. The thin line on the right side indicates *Qce$_c$-4BL*, the genomic region that is significantly associated with citrate efflux ($P < 0.05$). The solid bold line indicates the genomic region for *Qce$_c$-4BL* that is highly significantly associated with citrate efflux ($P < 0.001$). The numbers on the right side refer to linkage distance in centimorgans. Variation in citrate efflux was calculated as a percentage of the Carazinho donor parent.

wheat, but the degree of protection is smaller than that provided by malate efflux. This is demonstrated in Figure 8B, where Egret/Carazinho $F_{2:3}$ families, which are null for citrate efflux but homozygous for malate efflux, are significantly more resistant to 10 μM $AlCl_3$ than the $F_{2:3}$ family 30, which is homozygous for the citrate efflux phenotype but null for malate efflux. It is important to note that Al resistance in this study was measured at a single pH. The relative effectiveness of citrate and malate efflux in protecting plants from Al stress will also vary with external pH due to the speciation of both Al ($Al^{3+} \leftrightarrow AlOH^{2+} + H^+ \leftrightarrow Al_2(OH)_2^+ + 2H^+$, etc.) and the organic anions ($citrate^{3-} + 3H^+ \leftrightarrow citrate^{2-} + 2H^+ \leftrightarrow citrate^- + H^+$, etc.).

The evidence to date indicates that citrate efflux is restricted to a relatively few highly resistant genotypes from Brazil, including Carazinho, Toropi, Maringa, and Trintecinco. Interestingly, this trait is not present in Fronteira, Veranopolis, and Petiblanco, which are either derived from those genotypes or are among their progenitors. Surveys are on-going to establish how widely this trait is distributed among other cultivars, landraces, and subspecies of wheat. Atlas 66 (USA) and BH1146 (Brazil) are two highly Al-resistant cultivars that have been widely used in genetic studies. Many of those studies conclude that Atlas 66 and BH1146 possess more than one resistance gene (see introduction). Because the ancestries of Carazinho, Atlas 66, and BH1146 have several genotypes in common (e.g. Polyssu, Alfredo Chaves 6, Fronteira), we investigated whether they also have similar resistance mechanisms (de Sousa, 1998). Although both Atlas 66 and BH1146 show the Al-activated malate efflux, neither shows citrate efflux. It appears that citrate efflux does not contribute to the strong resistance of these two genotypes. Instead, a recently identified locus on chromosome 3BL of Atlas 66 and a Chinese genotype FSW appears to be important (Zhou et al., 2007; Cai et al., 2008), and this could encode a third mechanism conserved among genetically diverse genotypes.

CONCLUSION

This study describes a second mechanism for Al resistance in wheat located on chromosome 4BL, a region of the genome not previously associated with this phenotype. We provide evidence that the trait is likely encoded by a member of the MATE family of genes, *TaMATE1*. These results provide physiological evidence that Al resistance in wheat is a multigenic trait encoding for different mechanisms. Finally, we have identified SSR markers that will allow the rapid introgression of this locus into elite breeding material.

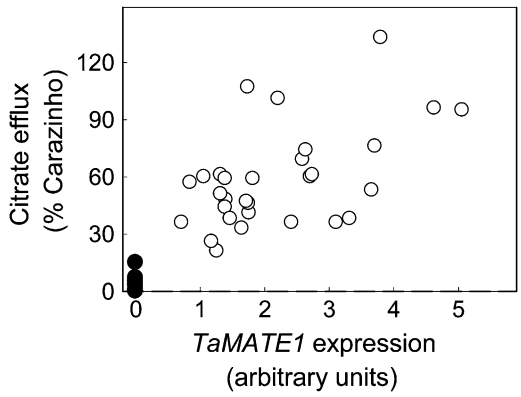

Figure 10. Relationship between *TaMATE1* expression and citrate efflux in $F_{2:3}$ families derived from Egret/Carazinho. *TaMATE1* expression in 3-mm root apices was measured by qRT-PCR and is shown relative to the expression of the wheat *PT-1* gene. Citrate efflux was assayed as described in the legend of Figure 7 and is expressed as a percent of Carazinho. White circles (○) indicate families that have detectable *TaMATE1* expression and black circles (●) are families with undetectable *TaMATE1* expression.

MATERIALS AND METHODS

Plant Material

Seeds for the genotypes investigated here were obtained from collections at CSIRO Plant Industry in Canberra, Australia, or from the Australian Winter Cereal Collection of the NSW Department of Primary Industries, Tamworth.

Parents of the segregating populations used in this study included Carazinho, an Al-resistant Brazilian wheat that carries the *TaALMT1-1* allele associated for Al resistance (Raman et al., 2008). Carazinho is derived from Polyssu/Alfredo Chaves 6//Fronteira/Mentana//Frontana/Egret. EGA-Burke (*TaALMT1-1* allele) is an Australian Al-resistant cultivar derived from Sunco and Hartog. The third parental line is Egret, an Al-sensitive cultivar (*TaALMT1-2* allele) with a pedigree of Heron/2*WW15. The F_2 population derived from EGA-Burke/Carazinho and 13 BC_1F_1 plants (EGA-Burke/Carazinho//EGA-Burke) were generated at CSIRO Plant Industry in Canberra, Australia. The 45 $F_{2:3}$ families derived from Egret/Carazinho were also generated at CSIRO Plant Industry.

Growth Conditions and Measurements of RRL

Seeds were germinated for 2 d on moist filter paper and then planted over 20 L of aerated nutrient solution (Delhaize et al., 2004) on laboratory benches. Seedlings were grown for 4 d before being used in experiments. To estimate RRL, the length of the longest root was measured before and after 4 d of growth in the same nutrient solution with a range of Al concentrations. RRL was calculated as (net root growth in Al treatment/net root growth in control solution) × 100. RRL could not be measured for single F_2 seedlings. Instead, net root growth was measured after 4 d in 30 μM Al treatment.

Measurement of Citrate and Malate Efflux

The measurement of organic anion efflux from intact seedlings followed the procedure of Delhaize et al. (1993b) and Ryan et al. (1995a). Briefly, seeds were surface sterilized with bleach and thoroughly rinsed in sterile water. Twelve seeds were placed in sterile conical flasks with 20 mL of 0.2 mM $CaCl_2$, pH 4.3, and kept on a rotary shaker. After 6 d, the solution was replaced with treatment solution, and aliquots were removed periodically for malate and citrate analysis. The concentration of malate and citrate were estimated with coupled enzyme assays that detect the production or consumption of NADH (Delhaize et al., 1993b; Wang et al., 2007).

Organic anion efflux from excised root apices could be measured on individual seedlings using as few as four apices by modifying the method described by Ryan et al. (1995a) and Wang et al. (2007). Briefly, approximately 4-mm root segments were excised in petri dishes and washed in 1 mL of control solution (0.2 mM $CaCl_2$, pH 4.3) for 1 h on a platform shaker (60 rpm). The solutions were replaced by 1 mL of treatments solution (with or without Al) and returned to the shaker for 1.5 to 2.5 h. For citrate measurements, samples were dried on a rotary vacuum drier and resuspended in 80 μL assay solution consisting of 100 mM Tris, pH 8.0, containing malate dehydrogenase (4 units), lactate dehydrogenase (1.5 units), and 15 μL NADH (prepared by dissolving 16 mg NADH and 15 mg $NaHCO_3$ in 2 mL water). The change in A_{340} was monitored after the reaction was initiated with citrate lyase (0.01 units). All chemicals were obtained from Sigma-Aldrich. Malate assay followed the procedure described by Ryan et al. (1995a). In some experiments, the samples were divided so that malate and citrate could be measured on the same sample. To gauge the efficiency of citrate recovery after drying, samples were spiked with known amounts of citrate. Approximately 40% of the citrate was unretrievable when citrate was dried in control solution (0.2 mM $CaCl_2$) and 60% was unretrievable when Al was present. These losses did not occur with malate, because the samples were not dried down prior to assaying. All data presented here show the corrected values for citrate efflux.

The variation observed between experiments probably relates to differences in the tissue to solution ratio, the length of the treatment, and laboratory environment (especially temperature). To account for this variation, Carazinho, and often Egret, were included in all experiments to act as internal standards. In some figures, the results are expressed as a percentage of Carazinho measured in the same experiment.

Genetic Mapping of Citrate Efflux

Leaf tissue was excised from each F_2 line after phenotyping for citrate efflux. Tissue samples were frozen in liquid nitrogen and pulverized using a Mixer-Mill (Retsch). Genomic DNA was extracted using a standard phenol-chloroform method. For the Egret/Carazinho population, genotypes of the F_2 parents for each $F_{2:3}$ family were reconstituted for mapping purposes by extracting DNA from bulks of leaf tissue from eight individual $F_{2:3}$ seedlings.

Qualitative (Xce_c) and quantitative (Qce_c) scores were used for mapping citrate efflux on the wheat genome. Xce_c was mapped by whole-genome mapping of 67 F_2 lines derived from EGA-Burke/Carazinho. Whole-genome profiling was performed using a DArT microarray chip (version 2.3) that contained approximately 5,000 unique DArT clones (www.triticarte.com.au). Twenty-five F_2 lines were randomly selected and replicated to determine the accuracy of DArT marker scores. DArT marker analysis was conducted as described previously (Akbari et al., 2006). Clones with a call rate >80% and 98% to 100% allele-calling concordance across the replicated assays were selected for mapping. The score of all segregating DArT markers were converted into 'A' and 'B' according to allele scores of the parental genotypes.

A skeleton linkage map was constructed with the Map Manager program, version QTX20b (Manly et al., 2001) using the Kosambi function (Kosambi, 1944). This map was subsequently employed to identify genomic region(s) associated with citrate efflux in an F_2 population from EGA-Burke/Carazinho using simple and interval mapping analyses as described in Manly et al. (2001). Accuracy of the order for DArT and SSR markers was checked with the RECORD computer package (Van os et al., 2005) and previously published maps (Akbari et al., 2006; www.triticarte.com.au).

Quantitative data on citrate efflux (relative to Carazinho) was used for QTL identification. Significance thresholds for the test statistics were estimated by 1,000 permutations at the significance of $P = 0.001$ (Churchill and Doerge, 1994; Doerge and Churchill, 1996) by following the algorithm implemented in Map Manager. The genomic region and chromosomal location associated with citrate efflux was designated as Qce_c-*4BL*.

SSR markers specific to chromosome 4B were tested for their association with Xce_c (Roder et al., 1998; Pestova et al., 2000; Guyomarc'h et al., 2002; Somers et al., 2004; Sourdille et al., 2004; Song et al., 2005). Markers *Xgwm251*, *Xgwm513*, *Xgwm495*, *Xcfd54*, *Xwmc48*, *Xwmc349*, *Xbarc340*, *Xcfd39*, *Xgwm165*, *Xgwm538*, *Xbarc163*, and *Xdupw43* were tested for polymorphisms between the parental lines Carazinho and EGA-Burke. Polymorphic markers were subsequently analyzed in each individual of an F_2 population. PCR amplifications were performed in 10-μL volumes on a Gene Amp PCR system 2700 (Applied Biosystems) thermal cycler using a touch-down PCR program (annealing temperature 65°C to 55°C with a decrease of 1°C for 10 cycles) as described previously by Raman et al. (2005). The 5′ end of the forward primer from each primer pair was tailed with a 19-nucleotide-long M13 sequence. Amplicons generated with fluorescent-labeled primers were analyzed using capillary electrophoresis on a CEQ8000 genetic analysis system (Beckman Coulter) as described by Raman et al. (2005). The score of SSR markers were converted into 'A' (homozygous for Carazinho), 'B' (homozygous for EGA-Burke), and 'H' (heterozygous allele from Carazinho and EGA-Burke). An integrated map based upon DArT and SSR loci was constructed using the RECORD program (Van os et al., 2005).

Quantitative citrate efflux data from an individual F_2 plant were binned into three categories according to their percentage of Carazinho: low (0%–27%), medium (36.4%–71.2%), and high (>71.2%). These scores were then converted into B, H, and A representing low, medium, and high citrate efflux phenotypes to predict homozygous and heterozygous alleles from EGA-Burke and Carazinho. Chi-square tests were performed on 67 F_2 lines to determine the goodness-of-fit of the phenotypes and markers into Mendelian segregation ratios. Citrate efflux and codominant SSR markers were used for linkage analysis using the Map Manager program. Linkage between citrate efflux and molecular marker(s) was determined at a threshold of $P = 0.001$. Map distances were calculated using the Kosambi function (Kosambi, 1944). Preferred orders of markers relative to Xce_c were checked by the "ripple" command within the Map Manager and the RECORD program. These linkage data were exported into Map Chart package (Voorrips, 2002) to display the trait-marker data graphically.

Measurements of *TaMATE1* Expression by Real-Time qRT-PCR

The expression level of a putative *MATE* gene from wheat (*TaMATE1*) was analyzed by qRT-PCR using procedures based on those described by Delhaize et al. (2004). RNA from 4-mm root tips was extracted with an RNeasy kit and used to synthesize first-strand cDNA, which was then diluted 64-fold prior to qRT-PCR. Primers GATTGCCGCGACCTCTCGTGTT (forward) and

GATGCCGTCGAACACGAACG (reverse) were used to amplify a 199-bp fragment from the cDNA by qRT-PCR. Expression of a phosphate transporter gene (*PT1*; GenBank accession no. AF110180; primers GAAGGACATCTTCACGGCGATC and CACGGCCATGAAGAAGAAGC) was used as an internal reference for each sample. PCR products were sequenced to confirm their identities. Data were analyzed by comparative quantification using Rotor-Gene software version 6.0 (Corbett Research), and expression of the *TaMATE1* gene was expressed relative to the expression of the *PT1* reference gene.

Sequence data from this article can be found in the GenBank/EMBL data libraries under accession numbers BE605049, BE498331, and AF110180.

Supplemental Data

The following materials are available in the online version of this article.

Supplemental Figure S1. Time course of malate and citrate efflux from excised root apices.

Supplemental Figure S2. Frequency distribution of citrate efflux in BC_1F_1 seedlings derived from EGA-Burke/Carazinho.

Supplemental Figure S3. Comparison of citrate efflux from Carazinho, Egret, and their F_1 progeny.

Supplemental Figure S4. A major QTL for citrate efflux maps to chromosome 4B.

Supplemental Figure S5. Endpoint products from qRT-PCR used to measure *TaMATE1* expression in $F_{2:3}$ families derived from a Carazhino by Egret cross.

Supplemental Table S1. Malate and citrate efflux from $F_{2:3}$ families derived from Egret/Carazinho.

ACKNOWLEDGMENTS

We are grateful to Dr. Rosy Raman, NSW DPI, Wagga Wagga, for the SSR analyses. The EH Graham Centre for Agricultural Innovation is an alliance between NSW Department of Primary Industries and Charles Sturt University, Wagga Wagga NSW, Australia.

Received September 2, 2008; accepted November 7, 2008; published November 12, 2008.

LITERATURE CITED

Akbari M, Wenzl P, Caig V, Carling J, Xia L, Yang S, Uszynski G, Mohler V, Lehmensiek A, et al (2006) Diversity arrays technology (DArT) for high-throughput profiling of the hexaploid wheat genome. Theor Appl Genet **113:** 1409–1420

Aniol A (1990) Genetics of tolerance to aluminum in wheat (*Triticum aestivum* L. Thell). Plant Soil **123:** 223–227

Aniol A, Gustafson JP (1984) Chromosome location of genes controlling aluminum tolerance in wheat, rye and triticale. Can J Genet Cytol **26:** 701–705

Berzonsky WA (1992) The genomic inheritance of aluminium tolerance in 'Atlas 66' wheat. Genome **35:** 689–693

Cai S, Bai GH, Zhang D (2008) Quantitative trait loci for aluminum resistance in Chinese wheat landrace FSW. Theor Appl Genet **117:** 49–56

Camargo CEO (1981) Wheat breeding. I. Inheritance of tolerance to aluminum toxicity in wheat. Bragantia **40:** 33–45

Churchill GA, Doerge RW (1994) Empirical threshold values for quantitative trait mapping. Genetics **138:** 963–971

Collins NC, Shirley NJ, Saeed M, Pallotta M, Gustafson JP (2008) An *ALMT1* gene cluster controlling aluminum tolerance at the *Alt4* locus of rye (*Secale cereale* L.). Genetics **179:** 669–682

de Sousa CNA (1998) Classification of Brazilian wheat cultivars for aluminum toxicity in acid soils. Plant Breed **117:** 217–221

Delhaize E, Craig S, Beaton CD, Bennet RJ, Jagadish VC, Randall PJ (1993a) Aluminum tolerance in wheat (*Triticum aestivum* L.) I. Uptake and distribution of aluminum in root apices. Plant Physiol **103:** 685–693

Delhaize E, Gruber BD, Ryan PR (2007) The roles of organic anion permeases in aluminium tolerance and mineral nutrition. FEBS Lett **581:** 2255–2262

Delhaize E, Ryan PR (1995) Aluminum toxicity and tolerance in plants. Plant Physiol **107:** 315–321

Delhaize E, Ryan PR, Hebb DM, Yamamoto Y, Sasaki T, Matsumoto H (2004) Engineering high-level aluminum tolerance in barley with the ALMT1 gene. Proc Natl Acad Sci USA **101:** 15249–15254

Delhaize E, Ryan PR, Randall PJ (1993b) Aluminum tolerance in wheat (*Triticum aestivum* L.) II. Aluminum stimulated excretion of malic acid from root apices. Plant Physiol **103:** 695–702

Doerge RW, Churchill GA (1996) Permutation tests for multiple loci affecting a quantitative character. Genetics **142:** 285–294

Fontecha G, Silva-Navas J, Benito C, Mestres MA, Espino FJ, Hernandez-Riquer MV, Gallego FJ (2007) Candidate gene identification of an aluminum-activated organic acid transporter gene at the Alt4 locus for aluminum tolerance in rye (*Secale cereale* L.). Theor Appl Genet **114:** 249–260

Furukawa J, Yamaji N, Wang H, Mitani N, Murata Y, Sato K, Katsuhara M, Takeda K, Ma JF (2007) An aluminum-activated citrate transporter in barley. Plant Cell Physiol **48:** 1081–1091

Garvin DF, Carver BF (2003) Role of genotypes tolerant of acidity and aluminium toxicity. *In* Z Rengel, ed, Handbook of Soil Acidity. Marcel Dekker Inc, New York, pp 387–406

Guyomarc'h H, Sourdille P, Charmet G, Edwards KJ, Bernard M (2002) Characterization of polymorphic microsatellite markers from *Aegilops tauschii* and transferability to the D genome of bread wheat. Theor Appl Genet **104:** 1164–1172

Hoekenga OA, Maron LG, Cançado GMA, Piñeros MA, Shaff J, Kobayashi Y, Ryan PR, Dong B, Delhaize E, Sasaki T, et al (2006) *AtALMT1,* which encodes a malate transporter, is identified as one of several genes critical for aluminium tolerance in Arabidopsis. Proc Natl Acad Sci USA **103:** 9738–9743

Hue NV, Craddock GR, Adams F (1986) Effect of organic anions on aluminum toxicity in subsoil. Soil Sci Soc Am J **50:** 28–34

Kerridge PC, Kronstad WE (1968) Evidence of genetic resistance to aluminum toxicity in wheat (*Triticum aestivum* Vill., Host). Agron J **60:** 710–711

Kinraide TB, Parker DR, Zobel RW (2005) Organic acid secretion as a mechanism of aluminium resistance: a model incorporating the root cortex, epidermis, and the external unstirred layer. J Exp Bot **56:** 1853–1865

Kochian LV, Hoekenga OA, Piñeros MA (2004) How do crop plants tolerate acid soils? Mechanisms of aluminum tolerance and phosphorous efficiency. Annu Rev Plant Biol **55:** 459–493

Kosambi DD (1944) The estimation of map distances from recombination values. Ann Eugen **12:** 172–175

Ligaba A, Katsuhara M, Ryan PR, Shibasaka M, Matsumoto H (2006) The *BnALMT1* and *BnALMT2* genes from *Brassica napus* L. encode aluminum-activated malate transporters that enhance the aluminum resistance of plant cells. Plant Physiol **142:** 1294–1303

Luo MC, Dvorak J (1996) Molecular mapping of an aluminum tolerance locus on chromosome 4D of Chinese Spring wheat. Euphytica **91:** 31–35

Ma HX, Bai GH, Carver BF, Zhou LL (2005) Molecular mapping of a quantitative trait locus for aluminum tolerance in wheat cultivar Atlas 66. Theor Appl Genet **112:** 51–57

Ma JF, Ryan PR, Delhaize E (2001) Aluminium tolerance in plants and the complexing role of organic acids. Trends Plant Sci **6:** 273–278

Ma JF, Zheng SJ, Matsumoto H (1997) Specific secretion of citric acid induced by Al stress in *Cassia tora* L. Plant Cell Physiol **38:** 1019–1025

Ma Z, Miyasaka SC (1998) Oxalate exudation by taro in response to Al. Plant Physiol **118:** 861–865

Magalhaes JV, Liu J, Guimaraes CT, Lana UGP, Alves VMC, Wang YH, Schaffert RE, Hoekenga OA, Piñeros MA, Shaff JE, et al (2007) A gene in the multidrug and toxic compound extrusion (MATE) family confers aluminum tolerance in sorghum. Nat Genet **39:** 1156–1161

Manly KF, Cudmore RH, Meer JM (2001) Map Manager QTX, cross-platform software for genetic mapping. Mamm Genome **12:** 930–932

Matsumoto H (2000) Cell biology of aluminum toxicity and tolerance in higher plants. Int Rev Cytol **200:** 1–46

Miyasaka SC, Buta JG, Howell RK, Foy CD (1991) Mechanisms of aluminum tolerance in snapbean. Plant Physiol **96:** 737–743

Papernik LA, Bethea AS, Singleton TE, Magalhaes JV, Garvin DF, Kochian LV (2001) Physiological basis of reduced Al tolerance in ditelosomic lines of Chinese Spring wheat. Planta **212:** 829–834

Pellet DM, Grunes DL, Kochian LV (1996) Multiple aluminum-resistance mechanisms in wheat. Roles for root apical phosphate and malate exudation. Plant Physiol **112:** 591–597

Pellet DM, Papernik LA, Kochian LV (1995) Organic acid exudation as an aluminum-tolerance mechanism in maize (*Zea mays* L.). Planta **196:** 788–795

Pestova E, Ganal MW, Roder MS (2000) Isolation and mapping of microsatellite markers specific for the D genome of bread wheat. Genome **43:** 689–697

Piñeros MA, Cançado GMA, Kochian LV (2008) Novel properties of the wheat aluminum tolerance organic acid transporter (TaALMT1) revealed by electrophysiological characterization in *Xenopus* oocytes: functional and structural implications. Plant Physiol **147:** 2131–2146

Polle E, Konzak CF, Kittrick JA (1978) Visual detection of aluminum tolerance levels in wheat by hematoxylin staining of seedling roots. Crop Sci **18:** 823–827

Raman H, Ryan PR, Raman R, Stodart BJ, Zhang K, Martin P, Wood R, Sasaki T, Yamamoto Y, Mackay M, et al (2008) Analysis of *TaALMT1* traces the transmission of aluminum resistance in cultivated common wheat (*Triticum aestivum* L.). Theor Appl Genet **116:** 343–354

Raman H, Zhang K, Cakir M, Appels R, Garvin DF, Maron LG, Kochian LV, Moroni JS, Raman R, Imtiaz M, et al (2005) Molecular mapping and characterization of *ALMT1*, the aluminium-tolerance gene of bread wheat (*Triticum aestivum* L.). Genome **48:** 781–791

Riede CR, Anderson JA (1996) Linkage of RFLP markers to an aluminum tolerance gene in wheat. Crop Sci **36:** 905–909

Roder MS, Korzun V, Wendehake K, Plaschke J, Tixier MH, Philippe L, Martin WG (1998) A microsatellite map of wheat. Genetics **149:** 2007–2023

Ryan PR, Delhaize E, Jones DL (2001) Function and mechanism of organic anion exudation from plant roots. Annu Rev Plant Physiol Plant Mol Biol **52:** 527–560

Ryan PR, Delhaize E, Randall PJ (1995a) Characterisation of Al-stimulated efflux of malate from the apices of Al-tolerant wheat roots. Planta **196:** 103–111

Ryan PR, Delhaize E, Randall PJ (1995b) Malate efflux from root apices and tolerance to aluminium are highly correlated in wheat. Aust J Plant Physiol **22:** 531–536

Ryan PR, DiTomaso JM, Kochian LV (1993) Aluminum toxicity in roots: investigation of spatial sensitivity and the role of the root cap in Al-tolerance. J Exp Bot **44:** 437–446

Ryan PR, Skerrett M, Findlay G, Delhaize E, Tyerman SD (1997) Aluminium activates an anion channel in the apical cells of wheat roots. Proc Natl Acad Sci USA **94:** 6547–6552

Sasaki T, Ryan PR, Delhaize E, Hebb DM, Ogihara Y, Noda K, Matsumoto H, Yamamoto Y (2006) Analysis of the sequence upstream of the wheat (*Triticum aestivum* L.) *ALMT1* gene and its relationship to aluminium tolerance. Plant Cell Physiol **47:** 1343–1354

Sasaki T, Yamamoto Y, Ezaki BB, Katsuhara M, Ahn SJ, Ryan PR, Delhaize E, Matsumoto H (2004) A wheat gene encoding an aluminum-activated malate transporter. Plant J **37:** 645–653

Sivaguru M, Horst WJ (1998) The distal part of the transition zone is the most aluminum-sensitive apical root zone of *Zea mays* L. Plant Physiol **116:** 155–163

Somers DJ, Gustafson JP (1995) The expression of aluminum stress induced polypeptides in a population segregating for aluminum tolerance in wheat (*Triticum aestivum* L.). Genome **38:** 1213–1220

Somers DJ, Isaac P, Edwards K (2004) A high-density microsatellite consensus map for bread wheat (*Triticum aestivum* L.). Theor Appl Genet **109:** 1105–1114

Song QJ, Shi JR, Singh S, Fickus EW, Costa JM, Lewis J, Gill BS, Ward R, Cregan PB (2005) Development and mapping of microsatellite (SSR) markers in wheat. Theor Appl Genet **110:** 550–560

Sourdille P, Singh S, Cadalen T, Brown-Guedira GL, Gay G, Qi L, Gill BS, Dufour P, Murigneux A, Bernard M (2004) Microsatellite-based deletion bin system for the establishment of genetic-physical map relationships in wheat (*Triticum aestivum* L.). Funct Integr Genomics **4:** 12–25

Stass A, Smit I, Eticha D, Oettler G, Horst WJ (2008) The significance of organic anion exudation for the aluminum resistance of primary triticale derived from wheat and rye parents differing in aluminum resistance. J Plant Nutr Soil Sci **171:** 634–642

Stodart BJ, Raman H, Coombes N, Mackay M (2007) Evaluating landraces of bread wheat *Triticum aestivum* L. for tolerance to aluminium under low pH conditions. Genet Resour Crop Evol **54:** 759–766

Tang Y, Garvin DF, Kochian LV, Sorrells ME, Carver BF (2002) Physiological genetics of aluminum tolerance in the wheat cultivar Atlas 66. Crop Sci **42:** 1541–1546

Taylor GJ (1988) The physiology of aluminum phytotoxicity. *In* H Sigel, A Sigel, eds, Metal Ions in Biological Systems, Vol 24. Marcel Dekker, New York, pp 123–163

Van os H, Stam P, Visser RGF, van Eck HJ (2005) SMOOTH: a statistical method for successful removal of genotyping errors from high-density genetic linkage data. Theor Appl Genet **112:** 187–194

von Uexküll HR, Mutert E (1995) Global extent, development and economic impact of acid soils. Plant Soil **171:** 1–15

Voorrips RE (2002) MapChart: software for the graphical presentation of linkage maps and QTLs. J Hered **93:** 77–78

Wang J, Raman H, Zhou M, Ryan PR, Delhaize E, Hebb DM, Coombes N, Mendham N (2007) High-resolution mapping of Alp, the aluminium tolerance locus in barley (Hordeum vulgare L.), identifies a candidate gene controlling tolerance. Theor Appl Genet **115:** 265–276

Yamaguchi M, Sasaki T, Sivaguru M, Yamamoto Y, Osawa H, Ahn SJ, Matsumoto H (2005) Evidence for the plasma membrane localization of Al-activated malate transporter (ALMT1). Plant Cell Physiol **46:** 812–816

Zhang WH, Ryan PR, Sasaki T, Yamamoto Y, Sullivan W, Tyerman SD (2008) Electrophysiological characterisation of the TaALMT1 protein in transfected tobacco (*Nicotiana tabacum* L.) cells. Plant Cell Physiol **49:** 1316–1330

Zhang WH, Ryan PR, Tyerman SD (2001) Malate-permeable channels and cation channels activated by aluminum in the apical cells of wheat roots. Plant Physiol **125:** 1459–1472

Zhao Z, Ma JF, Sato K, Takeda K (2003) Differential Al resistance and citrate secretion in barley (*Hordeum vulgare* L.). Planta **217:** 794–800

Zheng SJ, Ma JF, Matsumoto H (1998a) High aluminum resistance in buckwheat. I. Al-induced specific secretion of oxalic acid from root tips. Plant Physiol **117:** 745–751

Zheng SJ, Ma JF, Matsumoto H (1998b) Continuous secretion of organic acids is related to aluminum resistance during relatively long-term exposure to aluminium stress. Physiol Plant **103:** 209–214

Zhou LL, Bai GH, Ma HX (2007) Quantitative trait loci for aluminum resistance in wheat. Mol Breed **19:** 153–161